

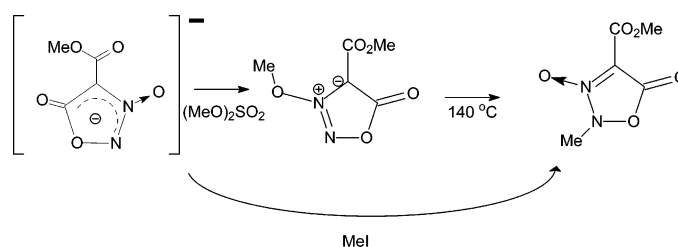
Methylation of Sydnone *N*-Oxides: Kinetic and Thermodynamic Control in the Alkylation Site of an Electron-Rich Heterocycle

D. Scott Bohle,* Lindsey E. McQuade, Inna Perepichka, and Lijuan Zhang

Department of Chemistry, McGill University, 801 Sherbrooke Street West,
Montreal, H3A 2K6, PQ, Canada

scott.bohle@mcgill.ca

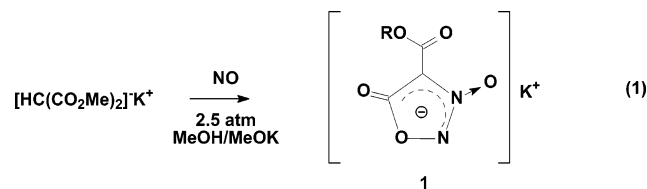
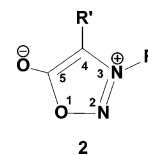
Received October 27, 2006



Methylation of the anionic 4-methylcarboxy 1,2,3-oxadiazolate 3-oxide occurs at either the disubstituted ring nitrogen or the oxygen of the *N*-oxide depending upon the conditions and reagents employed. Alkylation with methyl iodide leads to *N*-alkylation, while dimethyl sulfate gives *O*-alkylation and trifluoromethanemethylsulfonate gives a mixture of the two products. The regioselectivity of these methylations has been confirmed by X-ray diffraction of the two products, and these are in turn correlated with their theoretically predicted (B3LYP//6-311++G**) relative energies and vibrational spectra. Theoretically, *N*-alkylation is expected to give an isomer that is over 10 kcal mol⁻¹ more stable than the *O*-alkylated product. As a neat melt the kinetic *O*-alkylation product cleanly isomerizes in 2 h when heated to 140 °C to give the thermodynamic *N*-methylated isomer. Taken together the results illustrate the remarkable new sydnone *N*-oxide derivatives which are readily accessed in this chemistry, with the *N*-alkylation of the sydnone *N*-oxide, corresponding to the first case of such an *N*-alkylation for a diazenium diolate.

Introduction

We recently described a new synthetic approach to the sydnone heterocycle with its five-member 1,2,3-oxadiazole core.¹ In this synthesis nitric oxide addition to dimethyl malonate allows for the facile preparation of 4-carboxylate-substituted sydnone *N*-oxide, **1**, eq 1. These new anions have surprisingly



different reactivity than do the more well-studied sydnones, **2**.²

(1) Arulsamy, N.; Bohle, D. S. *Angew. Chem., Int. Ed.* **2002**, *41*, 2089–2091.

(2) Stewart, F. H. C. *Chem. Rev.* 1964, *64*, 129–147.

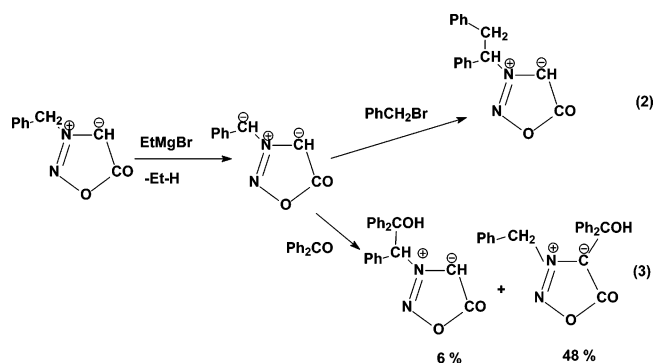
In particular the *N*-oxides are remarkably acid and base stable and show little tendency to react with dipolarophiles.³ They are also unusual diazeniumdiolates as they have an E geometry instead of the almost exclusively observed Z geometry.^{4–6} Since our initial discovery of **1**, related sydnone *N*-oxides have been prepared by the addition of nitric oxide to lithiated terminal

(3) Arulsamy, N.; Bohle, D. S.; Perepichka, I. *Can. J. Chem.* **2007**, *85*, 105–117.

(4) Keefer, L. K.; Flippen-Anderson, J.; George, C.; Shanklin, A. P.; Dunams, T. M.; Christodoulou, D.; Saavedra, J. E.; Sagan, E. S.; Bohle, D. S. *Nitric Oxide* **2001**, *5*, 377–394.

(5) Saavedra, J. E.; Bohle, D. S.; Smith, K. N.; George, C.; Deschamps, J. R.; Parrish, D.; Ivanic, J.; Wang, Y.-N.; Citro, M. L.; Keefer, L. K. *J. Am. Chem. Soc.* **2004**, *126*, 12880–12887.

alkynes.⁷ Prior synthetic approaches to sydnones are limited to a single sequence of nitrosation followed by cyclodehydration of 2-aminocarboxylates.² Naturally this has also limited the number and types of sydnones, their substituents, and thus the observed reactivity trends. For the parent heterocycle with $R' = H$, many electrophiles add to the 4 position by an aromatic electrophilic substitution.² Thus the 4-carbon position in 3-phenylsydnone has been nitrated,⁸ brominated,⁹ and sulfonated¹⁰ through electrophilic addition and proton loss at this carbon. On the other hand, for 4-substituted sydnones, with $R' = \text{alkyl}$ or aryl , electrophilic addition generally requires either prior metalation¹¹ or the use of strong acids such as $\text{FSO}_3\text{H}-\text{SbF}_5$.¹² For the anion generated from the metalation of 3-benzylsydnone with ethylmagnesium bromide the site of subsequent electrophilic addition depends upon the electrophile identity, with benzyl bromide leading to side chain benzylation, eq 2, and benzophenone giving predominately ring addition, eq 3.¹¹



We find that for the anionic sydnone *N*-oxides alkylation proves to be an important and facile reaction. Herein we report the following: (1) site and reagent specific methylation of sydnones with attack at either the oxygen of the *N*-oxide, to give **4**, or the nitrogen of the ring, to give **3**, depending upon the electrophile; (2) the conditions which lead to either (*N*)*O* or *N* methylation; (3) the facile isomerization of the kinetic product (**4**) with an $\text{NO}-\text{Me}$ linkage to the more thermodynamically stable product (**3**); (4) the demethylation kinetics of **4**; (5) the single-crystal X-ray diffraction structures for both of these products; and (6) density functional calculations to support these assignments and structures. Taken together this report also describes the first alkylation of a diazeniumdiolate at the disubstituted nitrogen.

Results and Discussion

Considering the negative charge of **1**, it should react readily with electrophiles, although the site of the electrophilic attack is not obvious and at least four different products could result

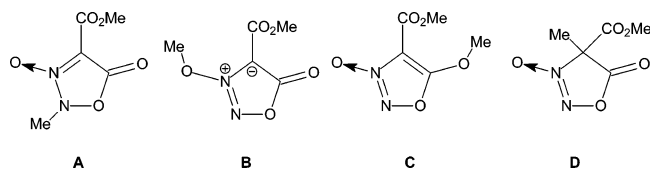
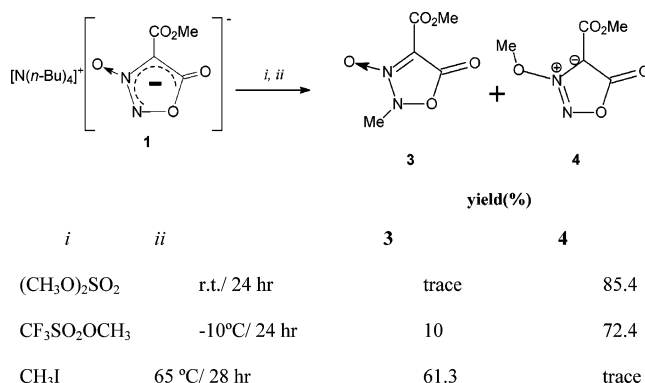


FIGURE 1. Possible methylation products of **1**.

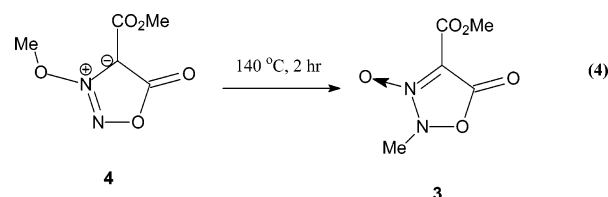
SCHEME 1. Products from the Methylation of **1**



(Figure 1). We examined the reaction of the tetra-*n*-butylammonium salt, **1**, prepared from its potassium salt by metathesis,³ with methyl iodide, dimethyl sulfate, and trifluoromethanemethylsulfonate, and observed the formation of two alkylated products, **3** (**A**) and **4** (**B**), in ratios depending on the reagent and reaction conditions (Scheme 1).

Thus, treatment of **1** with dimethyl sulfate or trifluoromethanemethylsulfonate produces preferentially *O*-methylated product **4**. However, reaction of **1** with methyl iodide affords the *N*-methylated derivative **3** as the major product. Although there is no indication of a photochemical effect, as a precaution these reactions were performed in the dark. Both products have been isolated and purified by flash chromatography and fully characterized by spectral methods, and their compositions and structures have been established by elemental analysis and X-ray diffraction.

When a neat melt of **4** is heated to 140°C for 2 h the predominant product is the *N*-methyl isomer **3**, eq 4. Thermoly-



sis of **3** under these conditions does not result in any detectable formation of **4** and higher temperatures lead to decomposition. Thus the isomer **4** corresponds to a kinetic product and **3** to a thermodynamic product. Attempts to monitor this isomerization in DMSO and alcohols result in methylation of the solvent and formation of the original anion **1**, i.e. the reverse of the equation shown in Scheme 1. The mechanism of the isomerization will be described latter.

In the course of these studies we also sought to specifically distinguish the anions with different ester groups. While it might at first appear that other malonate diesters would be useful for this task, for example, diethyl malonate instead of dimethyl malonate in eq 1, it is well-established that alcohols react readily

(6) Wang, Y.-N.; Bohle, D. S.; Bonifant, C. L.; Chmurny, G. N.; Collins, J. R.; Davies, K. M.; Deschamps, J. R.; Flippen-Anderson, J. L.; Keefer, L. K.; Klose, J. R.; Saavedra, J. E.; Waterhouse, D. J.; Parrish, D.; Ivanic, J. *J. Am. Chem. Soc.* **2005**, *127*, 5388–5395.

(7) Sugihara, T.; Kuwahara, K.; Wakabayashi, A.; Takao, H.; Imagawa, H.; Nishizawa, M. *Chem. Commun.* **2004**, 216–217.

(8) Weintraub, P. M.; Bambury, R. E. *Tetrahedron Lett.* **1969**, 579–581.

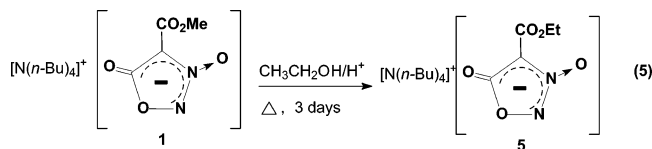
(9) Baker, W.; Ollis, W. D.; Poole, V. D. *J. Chem. Soc.* **1949**, 307.

(10) Yashchunskii, V. G.; Vasil'eva, V. F.; Sheinker, Y. N. *Zh. Obshch. Khim.* **1962**, *29*, 2712.

(11) Greco, C. V.; O'Reilly, B. P. *Tetrahedron Lett.* **1971**, 3057–3060.

(12) Olah, G. A.; Kelly, D. P.; Suci, N. *J. Am. Chem. Soc.* **1970**, *92*, 3133–3137.

with NO under these same conditions.¹³ To avoid complicating the reaction mixture with these possible side products we sought to determine the conditions for transesterification of the anion **1** to give its ethyl ester **5**, eq 5. An acid catalyst is used in



these reactions; clearly the stability of these sydnones in strong acid is an important reason why these conditions can be employed.³

Crystallographic Results

In common with the anionic sydnone *N*-oxides the new neutral methylated sydnone *N*-oxide derivatives **3** and **4** crystallize readily. Thus recrystallization is an ideal purification method for this family of compounds. Single crystals suitable for X-ray diffraction are directly obtained. Diffraction allows for the unambiguous structural assignment for the methylation products, and demonstrates that the thermodynamic methylation product **3** corresponds to the *N*-methyl sydnone *N*-oxide, **A**, while the kinetic methylation product, **4**, corresponds to the methoxysydnone derivative **B**. Crystallographic details for both structures are collected in the tables in the Supporting Information, with ORTEP representations for **3** and **4** shown in Figures 2 and 3. Table 1 contrasts the key experimental and theoretical metric parameters currently available for this family of compounds.

Common characteristics for all three structures are the marked planarity of their five-membered rings and the similarity of all the angles associated with the ring atoms. Perhaps the greatest variation in these structures is the bond lengths associated with the terminal oxygens O(1) and O(3). For the thermodynamic isomer **3** N(1)–O(1) and C(2)–O(3) are the shortest observed bond lengths. Thus strong N⁺–O[−] and C⁺–O[−] bonding modes are likely to significantly contribute to the stability of **3**. On the other hand, alkylation of O(1) to give the kinetic isomer **4** results in a product with a relatively short O(1)–N(1) bond. This in turn suggests that the sydnone anion is a good leaving group and that methyl exchange reactions should be facile, as is observed. While N(1)–N(2) is the shortest for the kinetic product **4** it is substantially longer ($\Delta = 0.136(9)$ Å) in the thermodynamic product **3**. These structural results suggest that in the balance of possible multibonding patterns in these rings that strong N(1)–O(1), C(2)–O(3), and N(1)–C(1) bonds will more than compensate for the loss of intraring multiple bonding by N(2). Another factor in these considerations is the pyramidal geometry found at N(2) in **3** where *N*-methylation results in a pyramidalization of the nitrogen with the angles at the nitrogen summing to 325°, which is slightly less than the expected sum for three angles in a tetrahedron of 327°.

Spectroscopic Characteristics. Prior vibrational spectroscopy of the sydnones has frequently discussed the implications of the extraannular carbonyl stretch $\nu(\text{C}=\text{O})$.² For the 4-methylcarboxylate esters **3** and **4** an unambiguous assignment of this band is complicated by coupling between the two vicinal $\nu(\text{C}=\text{O})$ modes, one from the extrannular carbonyl and the other

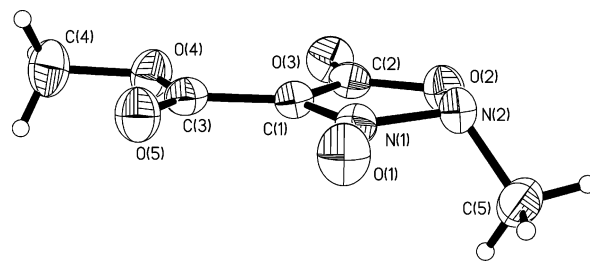


FIGURE 2. ORTEP representation of the thermodynamic methylation product **3**, which corresponds to an *N*-methylation of the sydnone *N*-oxide **1**.

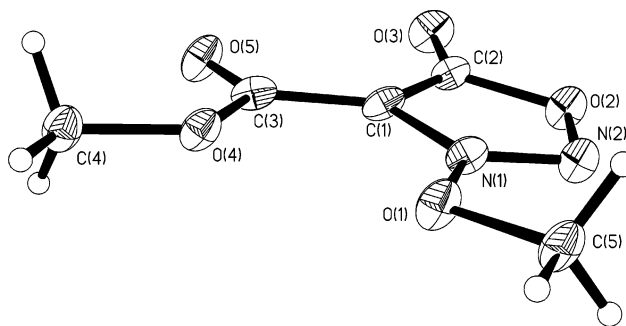


FIGURE 3. ORTEP representation of the kinetic methylation product **4** with an *O*-methylated sydnone *N*-oxide.

TABLE 1. Key Crystallographic and Theoretical Metric Parameters (Å and deg) for Structurally Characterized Sydnone *N*-Oxides

parameter	anion 1	4		3	
	exptl ^a	exptl ^b	theory ^c	exptl ^b	theory ^c
O(1)–N(1)	1.262(3)	1.350(2)	1.3560	1.240(2)	1.2220
N(1)–N(2)	1.324(3)	1.295(2)	1.2877	1.432(2)	1.4317
N(2)–O(2)	1.386(3)	1.383(2)	1.3484	1.422(2)	1.4088
N(1)–C(1)	1.380(3)	1.366(2)	1.3660	1.313(3)	1.3392
C(1)–C(3)	1.488(3)	1.452(2)	1.4618	1.476(3)	1.4774
C(1)–C(2)	1.405(3)	1.418(2)	1.4341	1.452(3)	1.4540
C(2)–O(3)	1.229(3)	1.209(2)	1.1892	1.186(3)	1.1908
C(2)–O(2)	1.367(3)	1.424(2)	1.4666	1.383(3)	1.4091
O(1)–N(1)–N(2)	118.35(19)	119.83(14)	116.04	115.72(19)	118.13
O(1)–N(1)–C(1)	130.2(1)	123.49(15)	127.0	132.9(2)	131.91
N(1)–N(2)–O(2)	106.6(1)	104.19(13)	105.11	104.24(16)	105.70
N(1)–N(2)–C(5)				112.32(18)	113.16
C(5)–N(2)–O(2)				109.06(17)	110.62

^a From ref 3. ^b This report. ^c Calculated with density functional theory, B3LYP/6-311++G**.

from the original $\nu(\text{CO}_2)_{\text{asym}}$. In addition to these bands a third band associated with the $\nu(\text{NO})$ for either the terminal *N*-oxide or the framework is present in the respective spectra of **3** and **4**, Tables 2 and 3. Although the overall ordering of the bands is predicted well with MP2 and DFT methods, the actual energies differ substantially for both **3** and **4** with the modes exhibiting strong coupling leading to 100 cm^{−1} calculated shifts for these three bands at both extremes for the midrange modes. We have examined the trends in these bands by using a range of methods for both **3** and **4**, Tables 2 and 3, and a range of basis sets from ζ to triple ζ in quality, Table 2. MP2 vibrational energies are often scaled to compare these values with experiment, but in our experience the DFT vibrational energies seldom require this manipulation.³ Apart from VWN correlation functional and the Perdew gradient corrected function P86 all of the DFT methods give significantly higher energies for the ν_{42} band than is found for experiment. It is interesting that

(13) Wieland, H.; Kerr, F. N. *Chem. Ber.* **1930**, 63, 570–579.

TABLE 2. Method and Basis Set Dependence for Experimental and Calculated Vibrational Frequencies Calculated for **3**

method	basis set	energy (hartrees, au)	midrange modes: ν_{42} , ν_{41} , and ν_{40} (cm ⁻¹)			
KBr			1877 w	1817 s	1726 s	1580 s
CH ₂ Cl ₂				1802 s		
MP2	6-311++G**	-678.110 690 14		1806 s	1739 s	1573 s
B3LYP	6-311++G**	-679.831 483 77	1867	1803	1783	
B3LYP	6-311+G*	-679.823 784 35	1895	1788		1605
B3LYP	6-311G	-679.569 815 13	1880	1785		1605
B3LYP	6-31G	-679.380 981 40		1798	1638	1537
B3PW91	6-311++G**	-679.562 680 33	1830		1706	1556
B3P86	6-311++G**	-681.437 931 10	1901	1809		1641
BP86	6-311++G**	-679.870 930 09	1905	1813		1645
BW91/PW91	6-311++G**	-679.653 613 86	1818		1720	1571
BVWN	6-311++G**	-684.356 936 26		1831	1730	1583
				1791	1699	1531

TABLE 3. Method and Basis Set Dependence for Experimental and Calculated Vibrational Frequencies Calculated for **4**

method	basis set	energy (hartrees, au)	midrange modes: ν_{42} , ν_{41} , and ν_{40} (cm ⁻¹)		
KBr			1800 s	1724 s	1491 s
CH ₂ Cl ₂			1805 s	1717 s	1490 s
MP2	6-311++G**	-678.098 916	1901	1785	1635
B3LYP	6-311++G**	-679.814 273 19	1906	1763	1377
B3PW91	6-311++G**	-679.544 181 24	1926	1780	1523
B3P86	6-311++G**	-681.409 553 38	1930	1794	1529
BP86	6-311++G**	-679.851 524 94	1860	1704	1451
BVWN	6-311++G**	-684.339 163 24	1845	1678	1486

TABLE 4. Calculated Energies for Ground and Transition States for the Isomers of d[MeO₂CCN(O)=NOC(O)]Me

structure	energy (au)	rel energy (kcal/mol)
3 (A) thermodynamic	-679.830 456 44	0
4 (B) kinetic	-679.814 273 19	10.2
C	-679.798 411 2	20.1
D	-679.819 903 2	6.6
TS 1, 1,3 methyl shift	-679.705 933 24	78.1
TS 2, N-inversion	-679.820 648 9	6.2

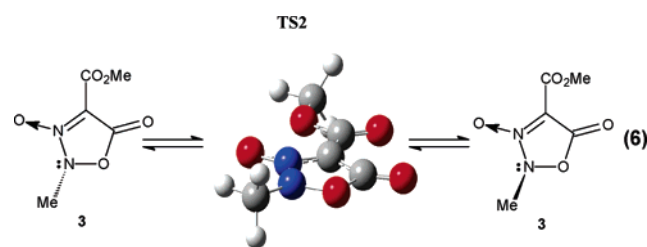
the hybrid DFT methods such as B3LYP, which are now well established and have a remarkable track record for predicting these properties in small closed shell organic derivatives, should overestimate the strength of these modes. We speculate that it may be a consequence of the mesoionic character of these rings, and we note that related problems have been critically re-examined in multiply bound and charged metal systems which have closely spaced π and π^* levels.¹⁴ The solution spectra for **3** demonstrate some solid-state splitting of the methylcarboxylate band with the two strong bands at 1817 and 1802 cm⁻¹ in the solid being reduced to a single band at 1806 cm⁻¹ in dichloromethane.

Theoretical Studies. To shed light on the observed reactivity of sydnone **1**, we performed theoretical calculations using density functional theory with triple ζ basis sets (B3LYP/6-311++G**) for each of the possible methylation products **A–D**. Detailed geometries for each of these stationary points are listed in the Supporting Information along with their key vibrational frequencies. In general all isomers **A–D** share a common nearly planar five-member ring in which all have some degree of delocalized π -bonding. Since the four proposed ground states are neutral structural isomers with the same numbers of electrons and atoms it is possible to directly compare their gas-phase calculated energies, Table 4.

Of the four putative isomers **A–D** that have been shown to correspond to ground-state minima, there is evidence for the

presence of only two, **A** and **B** in the methylation reactions. Even though C-methylation at the 4-position, to give **D**, results in a theoretically more stable isomer than **B**, it is not observed. TLC analysis of the reaction products indicates that apart from minor decomposition there are no other products in these reactions.

In considering the reactions of **3** and **4** we examined the potential energy surfaces for the low-lying transition states for their interconversion and isomerization. Not surprisingly the lowest lying transition state for isomerization, TS 2 in Table 4, corresponds to nitrogen inversion, eq 6. This low-lying inversion



transition state is similar to those found experimentally and theoretically for related annulated nitrogen inversions.^{15–17} Perhaps more interesting is the observed isomerization of **4** to **3** which, if it occurs *intramolecularly*, would involve a^{1,3} sigmatropic rearrangement or O to N methyl shift. From Woodward–Hoffmann rules the orbital symmetry allowed transition state should be 2s + 2a, which in this case would correspond to the two lobes of the p-orbital on the sp² hybridized methyl interacting with the N–N–O group.¹⁸ With the synchronous transit guided quasi-newton (STQN)¹⁹ algorithm implemented in Gaussian-98 a transition state with the allowed 2s + 2a geometry is located, Figure 4, albeit almost 70 kcal mol⁻¹ above the ground-state energy of the kinetic isomer, Table

(15) Brouwer, A. M.; Krijnen, B. *J. Org. Chem.* **1995**, *60*, 32–40.

(16) Nielsen, I. M. B. *J. Phys. Chem. A* **1998**, *102*, 3193–3201.

(17) Lehn, J. M. *Fortschr. Chem. Forsch.* **1970**, *15*, 311–377.

(18) Berson, J. A. *Acc. Chem. Res.* **1972**, *5*, 406–414.

(19) Peng, C.; Schlegel, H. B. *Isr. J. Chem.* **1994**, *33*, 449.

(14) Petrie, S.; Stranger, R. *Inorg. Chem.* **2004**, *43*, 2597–2610.

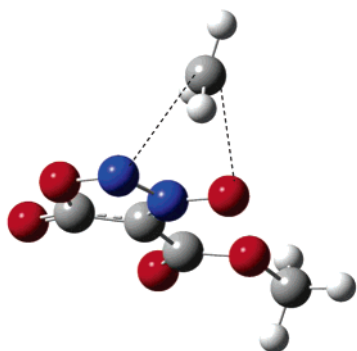


FIGURE 4. Transition state TS1 for the allowed intramolecular 2s + 2a rearrangement of **4** to **3**.

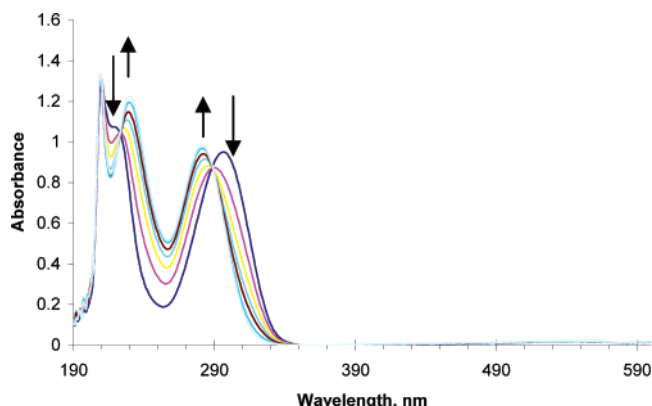
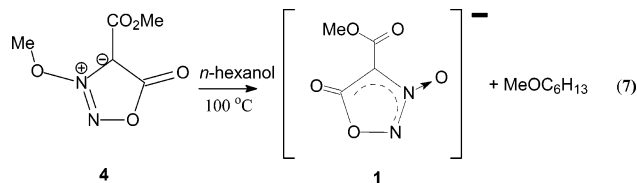


FIGURE 5. Demethylation of **4** by *n*-hexanol at 100 °C to give **1**. The time interval between scans is 500 s.

4. Taken together the high-energy barrier and the relatively fast observed kinetics for the isomerization and demethylation reactions of **4** suggest that a nonconcerted *intermolecular* mechanism might be responsible for the isomerization of **4** to **3**.

Kinetics for the Isomerization and Demethylation of 4. With a neat melt at 140 °C **4** is converted to **3** within 2 h. At higher temperatures there is considerable decomposition of **3**, which complicates the kinetics. The isomerization occurs cleanly with only minor decomposition and accumulation of side products as determined by NMR spectroscopy. In this melt the effective concentration is likely to be at least 6 M, and we sought to find a method to measure these kinetics at different concentrations. Unfortunately all attempts to monitor the kinetics of the isomerization of **3** to **4** in *n*-hexanol, DMSO, and DMF have resulted in clean demethylation of **4** to return the anion **1**, eq 7. For example, the reaction of **4** with *n*-hexanol at 100 °C



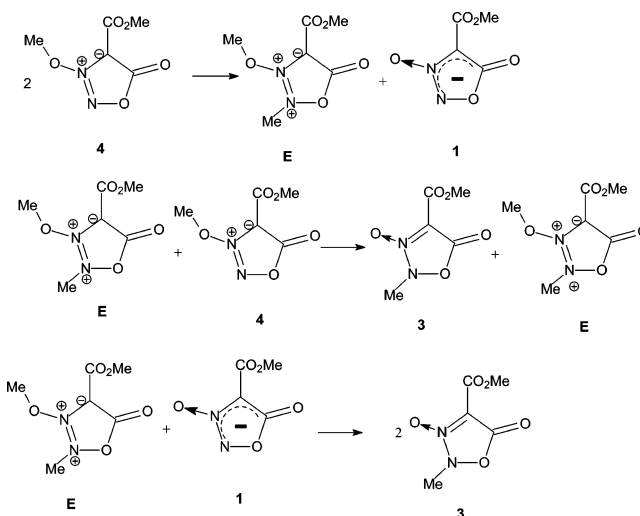
has been followed by UV spectroscopy, Figure 5. Although the reaction is clearly isosbestic the product has bands at 230 and 281 nm, identical with the anion **1** in *n*-hexanol.

In DMSO the demethylation is considerably more rapid and occurs at lower temperatures. We have used ¹H NMR in DMSO-

TABLE 5. Kinetics Data for the Demethylation of **4** To Give **1** in DMSO-*d*₆

concn, M	$10^4 k_1, \text{s}^{-1}$
25 °C	
6×10^{-3}	0.63 ± 0.01
2.4×10^{-1}	0.63 ± 0.01
4.0×10^{-1}	0.70 ± 0.01
	$k_1 = 0.65(4) \text{ s}^{-1}$
40 °C	
6×10^{-3}	5.45 ± 0.05
1.7×10^{-2}	5.23 ± 0.05
2.9×10^{-2}	5.69 ± 0.03
	$k_1 = 5.5(2) \text{ s}^{-1}$
50 °C	
6.4×10^{-2}	8.27 ± 0.01
2.0×10^{-1}	7.91 ± 0.02
2.9×10^{-1}	8.16 ± 0.03
	$k_1 = 8.1(2) \text{ s}^{-1}$

SCHEME 2. Possible Demethylation Mechanisms for **4**



*d*₆ to follow the demethylation kinetics of **4** at several temperatures to give **1** and have found that the reaction is first order in **4**, with a rate constant independent of the concentration of **4**, and has only a negative but modest entropy of activation of ca. $-10 \text{ cal mol}^{-1} \text{ K}^{-1}$. Table 5 collects the observed kinetics for the demethylation of **4**. From the Arrhenius plot (not shown) it is possible to extract the activation parameters of $\Delta E_a = 21.4 \text{ kcal mol}^{-1}$, $\Delta H^\ddagger = 20.8 \text{ kcal mol}^{-1}$, and $\Delta S^\ddagger = -7.8 \text{ cal mol}^{-1} \text{ K}^{-1}$. The most likely mechanism that explains these kinetics is that intermolecular methyl transfer to the solvent in the case of hexanol or DMSO is independent of the concentration of **4** and dominated by the large excess of solvent, which acts as the reagent. Attempts to dilute the DMSO ¹H NMR experiments with other solvents such as acetonitrile, or benzene, solvents that do not demethylate **4**, resulted in reactions too slow to observe by ¹H NMR for a period of over a week. On the other hand, as a neat melt we propose that there is still likely to be a rate-limiting *intermolecular* methyl transfer to give transient cations such as **E**, Scheme 2, which then engage in a rapid methyl transfer either back to the generated anion or to another unreacted **4**. Even when prolonged times and excess alkylating agents are used there is little evidence of the formation of a dimethylated charged species such as **E** being produced. In this scheme both **4** and especially **E** are methylating agents.

Alkylation of 2-N. Clearly the products of methylation are dependent upon the alkylating agent and conditions, with two

new heterocycles resulting from alkylating either the ring nitrogen or the oxygen of the *N*-oxide. The sydnone *N*-oxide **1** is an unusual and rare example of an *E*-diazoniumdiolate, most of the known species adopt a *Z* geometry.¹ Reactions of the *Z*-diazoniumdiolates almost never involve the two-coordinate nitrogen, even though Lewis diagrams formally localize a lone pair of electrons at this center. A possible conclusion one can draw is that in the *Z*-geometry this lone pair is very low in energy, or strongly delocalized, and so it cannot be alkylated or coordinated.²⁰ Why does this reactivity seem to change when the diazeniumdiolate adopts an *E* geometry, as in **1**? To answer this question unambiguously we are currently searching for new examples of the alkylation of noncyclized diazeniumdiolates.

Conclusions

The sydnone *N*-oxide anion is an ambident nucleophile with a number of possible alkylation sites. Alkylation of the *N*-oxide oxygen returns a kinetic product, **A**, which can be readily demethylated or isomerized to the thermodynamically stable *N*-methylation product, **B**. Although in prior work we have demonstrated coordination through the carbonyl oxygen of the annulated carbonyl, there is no evidence that this oxygen can be alkylated under the conditions reported here. Electrophilic addition to the carbon at the 4-position on the ring has also not been observed with these methylating electrophiles. The alkylation of the nitrogen at the 2 position is particularly striking as this is the first report of the *N*-alkylation of a diazeniumdiolate.

Experimental Section

The potassium and tetra-*n*-butylammonium salts of 3-carboxymethylsydnone-*N*-oxide, **1**, were prepared by reaction of nitric oxide with dimethyl malonate, as previously reported, followed by cation methathesis.³

Preparation of *N*-Methyl 4-Methylcarboxysydnone *N*-Oxide, the Thermodynamic Methylation Product (3). A mixture of 0.40 g (0.10 mmol) of **1** with 1.42 g (1.00 mmol) of methyl iodide in dry acetonitrile (5 mL) was heated to 65–70 °C in a closed medium-pressure glass reaction tube under nitrogen in the dark for 28 h. After cooling to room temperature 20 mL of water was added to the resulting mixture. The product was extracted with dichloromethane, washed with brine, dried over magnesium sulfate, filtered, and concentrated in vacuo. The residue was purified on silica gel, using hexane/ethyl acetate (1:1, v/v) as an eluent; yield 0.106 g (61.2%, from dichloromethane/hexane) of compound **3** and only a trace of compound **4**. Characteristic data for **3**, which is isolated as a colorless crystalline solid: Mp 51–52 °C (from dichloromethane/hexane). ¹H NMR (300 MHz, CDCl₃, ppm): δ 3.49 (s, 3H, CH₃-N), 3.98 (s, 3H, CH₃-O). ¹³C NMR (300 MHz, CDCl₃, ppm): δ 45.5, 53.5, 107.7, 155.8, 159.2. IR (KBr, cm⁻¹): 3024 w, 2962 w, 1877 w, 1817 s, 1802 s, 1726 s, 1580 s, 1465 m, 1443 s, 1414 m, 1392 m, 1239 m, 1082 m, 1017 m, 977 w, 930 w, 857 w, 780 w, 774 m, 722 w, 688 w, 669 m, 642 m, 624 w, 422 w. UV (CH₃OH λ_{max}, nm (ε, M⁻¹ cm⁻¹)): 261 (8570), 285 (sh), 315 (sh). MS (ESI), *m/z*: calcd for C₅H₆N₂O₅ [M]⁺ 174, found [M + Na]⁺ 197 (100%). Anal. Calcd for C₅H₆N₂O₅ (174 g/mol): C, 34.49; H, 3.47; N, 16.08. Found: C, 34.63; H, 3.18; N, 15.84.

Preparation of *O*-Methyl 4-Methylcarboxysydnone *N*-Oxide, the Kinetic Product (4). A solution of the salt **1** (0.70 g, 1.75 mmol) in dry acetonitrile (10 mL) was cooled to –10 °C under nitrogen. While stirring, 0.315 g (1.92 mmol) of methyl trifluoro-

methanemethylsulfonate was added via a syringe and the reaction mixture was kept cold in the dark. After 1 h the reaction mixture was allowed to warm to ambient temperature and left overnight. The solvent was evaporated and the residue was dissolved in 40 mL of methylene chloride, washed with aqueous 10% solution of sodium bicarbonate (30 mL), water (2 × 20 mL), and brine (2 × 30 mL), and dried over magnesium sulfate. After removal of the solvent the crude product was purified by column chromatography on silica gel with hexane/ethyl acetate (1:1, v/v) as an eluent. The first band (*R*_f 0.60) yielded 0.03 g (10%) of compound **3** while the second band (*R*_f 0.30) gave 0.22 g (72.4%) of compound **4** as a white precipitate after addition of hexane: Mp 41–42 °C (from methylene chloride/hexane). ¹H NMR (300 MHz, CDCl₃): δ 3.89 (s, 3H, CH₃-OC), 4.51 (s, 3H, CH₃-ON). ¹³C NMR (300 MHz, CDCl₃, ppm): δ 52.8, 67.4, 93.9, 156.3, 162.3. IR (KBr, cm⁻¹): 2960 w, 1800 s, 1724 s, 1491 s, 1437 w, 1375 m, 1349 m, 1209 s, 1176 m, 1111 s, 1041 s, 936 m, 887 w, 801 m, 762 s, 620 w, 440 w. UV (CH₃OH λ_{max}, nm (ε, M⁻¹ cm⁻¹)): 296 (9500). MS (ESI), *m/z*: calcd for C₅H₆N₂O₅ [M] 174, found [(M – NO) + Na]⁺ 167 (30%), [M + Na]⁺ 197 (100%). Anal. Calcd for C₅H₆N₂O₅ (174 g/mol): C, 34.49; H, 3.47; N, 16.08. Found: C, 34.48; H, 3.22; N, 15.97.

Alkylation of **1 with Dimethyl Sulfate.** To a solution of **1** (0.188 g, 0.469 mmol) in dry acetonitrile (5 mL) under nitrogen at room temperature was added 0.192 g (1.52 mmol) of freshly distilled dimethyl sulfate via a syringe. After the solution was stirred overnight in the dark the solvent was removed and the residue was taken up in dichloromethane and washed with 5% aqueous sodium hydroxide solution. The organic phase was washed with water and brine, dried over magnesium sulfate, filtered, and concentrated in vacuo. The crude product was purified by column chromatography on silica gel with hexane/ethyl acetate (1:1, v/v) as an eluent and recrystallized from dichloromethane/hexane yielding 0.07 g (85.4%) of compound **4**. Compound **3** was not isolated in this reaction.

Isomerization of the Kinetic Product **4 into **3**: As a Neat Solid Melt.** Compound **4** (0.03 g) was inserted under nitrogen into a dry NMR tube that closed with a cap and sealed with Parafilm. The tube was placed in a preheated oil bath (140 °C). After being kept at this temperature for 2 h the sample was allowed to cool to 20 °C and dissolved in chloroform-*d*₁. The NMR spectra, ¹H and ¹³C, clearly indicated complete and clean conversion of compound **4** into **3**.

Transesterification of Tetra-*n*-butylammonium 4-Methylcarboxysydnone *N*-Oxide **1 into Its Ethyl Ester **5**.** A solution of **1** (0.15 g, 0.374 mmol) and *p*-toluenesulfonic acid monohydrate (10–15 mol %) in ethanol (10–15 mL) was stirred at reflux for 3 days (reaction progress was monitored by ¹H NMR in CDCl₃). After the solution was cooled to room temperature the solvent was evaporated and the residue was dissolved in 40 mL of methylene chloride. The extract, after being washed with an aqueous 10% solution of sodium bicarbonate (30 mL), water (3 × 20 mL), and brine (2 × 30 mL) and dried over magnesium sulfate, was evaporated to furnish **5** as a white crystalline solid. Yield 0.10 g (65%), mp 97–98 °C. ¹H NMR (300 MHz, CDCl₃, ppm): δ 0.99 (t, 12H, *J* = 7.4 Hz, CH₃-Bu), 1.30–1.47 (m, 3H CH₃-ester; 8H, CH₂-Bu), 1.63 (quint, 8H, *J* = 8 Hz, CH₂-Bu), 3.23 (t, 8H, *J* = 8 Hz, CH₂-Bu), 4.30 (q, 2H, *J* = 7 Hz, CH₂-ester). ¹³C NMR (400 MHz, CDCl₃, ppm): δ 13.6, 14.7, 19.7, 23.9, 58.7, 59.2, 95.0, 159.7, 166.6. UV (CH₃OH λ_{max}, nm (ε, M⁻¹ cm⁻¹)): 228 (13 640), 277 (10 380). MS (ESI): *m/z* calcd for [C₄H₃N₂O₅][N(C₄H₉)₄] [M] 415, found [N(C₄H₉)₄]⁺ 242 (100%), [M + [N(C₄H₉)₄]]⁺ 657 (8%), [M – [N(C₄H₉)₄]][–] 173 (100%), [2M – [N(C₄H₉)₄]][–] 588 (68%). Elemental analysis calcd for C₂₁H₄₁N₃O₅ (415 g/mol): C, 60.69; H, 9.94; N, 10.11. Found: C, 60.29; H, 9.83; N, 9.86.

Computational Details. All of the calculations described above were performed with Gaussian 98.²¹ We have studied the two

(20) Arulsamy, N.; Bohle, D. S.; Imonigie, J. A.; Sagan, E. S. *J. Am. Chem. Soc.* **2000**, *122*, 5539–5549.

(21) Frisch, M. J.; et al. *Gaussian 98*; Gaussian Inc.: Pittsburgh, PA, 1998.

neutral methylation products **3** and **4** as well as the transition states for nitrogen inversion and intramolecular 1,3-methyl shift. In each case, the optimized structures were determined. Computations were carried out at the restricted Hartree–Fock (RHF),²² and Density Functional Theory (DFT). DFT calculations used the hybrid B3LYP functional and triple- ζ 6-311++G** basis sets.^{22–24} Vibrational frequencies were calculated for all stationary points to define them as either minima or transition states.

X-ray Crystallography. Single-crystal X-ray diffraction experiments were carried out with a BRUKER SMART CCD diffractometer, using graphite-monochromated Mo K α radiation ($\lambda = 0.71073$ Å). The structures were solved by direct methods and refined by full-matrix least-squares on F^2 of all data, using

(22) Roothaan, C. C. *J. Rev. Mod. Phys.* **1951**, 23, 69–89.

(23) Lee, C. Y., W.; Parr, R. G. *Phys. Rev. B* **1988**, 37, 785–789.

(24) Becke, A. D. *J. Chem. Phys.* **1993**, 98, 5648–5652.

SHELXTL software.²⁵ Key crystallographic data are summarized in Table S1 (Supporting Information).

Acknowledgment. We gratefully acknowledge the CRC, CFI, and NSERC for support in the forms of a CRC, CFI, and discovery grant to D.S.B., and Summer Research Fellowship to L.M., and to the CIHR for a Chemical Biology Fellowship to Dr. Inna Perepichka.

Supporting Information Available: Crystallographic data (CIF files) and density functional calculation results for **3** and **4** and their possible isomers. This material is available free of charge via the Internet at <http://pubs.acs.org>.

JO062235K

(25) *SHELXTL* 5.10 ed.; Bruker AXS, Inc.: Madison, WI, 1997.